DEUTSCHES ELEKTRONEN-SYNCHROTRON DESY

DESY SR 85-09
September 1985

OUTPUT DIAGNOSTICS OF THE GRAZING INCIDENCE PLANE GRATING MONOCHROMATOR BUMBLE BEE (15-1500 eV)

by

W. Jark

II. Institut f. Experimentalphysik, Universität Hamburg

C. Kunz

II. Institut f. Experimentalphysik, Universität Hamburg
and
Hamburger Synchrotronstrahlungslabor HASYLAB at DESY

ISSN 0723-7979

NOTKESTRASSE 85 · 2 HAMBURG 52

To be sure that your preprints are promptly included in the
HIGH ENERGY PHYSICS INDEX ,
send them to the following address (if possible by air mail) :

DESY
Bibliothek
Notkestrasse 85
2 Hamburg 52
Germany

DESY SR 85-09
September 1985

ISSN 0723-7979

OUTPUT DIAGNOSTICS OF THE GRAZING INCIDENCE PLANE GRATING MONOCHROMATOR BUMBLE BEE (15-1500 eV)

W. Jark and C. Kunz

II. Institut für Experimentalphysik, Universität Hamburg,
Luruper Chaussee 149, D-2000 Hamburg 50, and
HASYLAB-DESY, Notkestr. 85, D-2000 Hamburg 52

Abstract

The BUMBLE BEE is a bakeable UHV compatible plane grating monochromator with a fixed exit beam, and the capability to suppress higher order radiation in a wide energy range. The instrument was built to be used in connection with a UHV reflectometer and has a differential pumping section between the optical components and the sample allowing a pressure of 10^{-5} torr in the experimental chamber without influencing the UHV in the monochromator. The monochromator is not optimized for resolution. Due to its location at a beamline with a short source distance we achieve only medium resolving power in the order of $E/\Delta E \approx 200$. The primary goal is the suppression of higher orders, fortunately the thus selected operating parameters for the coupled rotations of the optical components also give nearly the highest available output. The instrument is characterized in great detail. The performance of the instrument is discussed and compared with extensive theoretical calculations.

- presented at SRI 85 in Stanford, CA, USA, July 29th - Aug. 2nd, 1985
to be published in Nucl. Instr. & Meth.

1. Introduction

Three years ago we presented the design principles /1/ of a new monochromator BUMBLE BEE capable of suppressing higher orders in a wide energy range. It goes back to the original GLEISPIMO design /2/ which was modified several times in the meantime. The monochromatization is achieved by a plane grating in combination with a paraboloid focussing into the exit slit as shown in Fig. 1. The beamline G1 as shown in Fig. 1 (the dimensions are given in detail in Table 1) consists of a 4° plane deflection mirror (PM1) in front of the monochromator, a plane premirror (PM) and a plane grating (PG), a focussing paraboloid (P) and the exi t slit (ES).

The BUMBLE BEE design /1/ is quite close to that of the SX700 at the BESSY laboratory /3,4/. In our concept the angle of incidence on a rotating premirror and on the independently rotatable grating is varied in such a way that the desired wavelength is enhanced with respect to the higher orders by making use of the cut-off for total reflection. The BUMBLE BEE is in use since July 1984 and provides VUV- and soft X-ray light in the range $0.8\ nm \leq \lambda \leq 80.0\ nm$ ($15\ eV \leq E \leq 1500\ eV$) for a UHV reflectometer /5/ having all the necessary installations to make precision measurements on reflected, scattered, and transmitted radiation. λ is the wavelength and E the photon energy.

Parallel to first systematic investigations of optical properties of plane mirrors and plane gratings a diagnosis of the monochromator output was made. We discuss here the performance of the instrument and compare the data with those originally predicted /1/ and with the results from recently improved computer simulations. The data presented are not primarily optimized for

output, but primarily for good suppression of higher orders, so that one can operate the reflectometer with almost pure monochromatized light.

2. Optimization of operating parameters

The first investigation with the reflectometer in combination with the new monochromator was measuring the efficiency of a plane blazed grating with a blaze angle $\gamma = 1.5°$ and groove density 1200/mm. It is quite similar to the grating in the BUMBLE BEE itself with a blaze angle $\gamma = 1.0°$ and groove density 1200/mm. This grating had been installed in the FLIPPER monochromator /6/ from April 1980 to November 1981 /7/. The original gold coating and the contamination layer were removed from the ion etched glass block and a new gold coating (30 nm thick) was evaporated. After this regeneration the original efficiency of 10 % at the carbon K-edge ($\lambda = 4.38$ nm) was restored. Fig. 2 was derived from the data measured between 1 nm $\leq \lambda \leq$ 20 nm. The curves e_{1max} for first order maximum efficiency and $e_{1max/2}$ for the 50 % level support the grating efficiency map introduced by Petersen /4/. We could have derived also similar diagrams for the second orders, but here we want to give a different presentation. We indicate those regions where the efficiency of the second order of $\lambda/2$ exceeds 10 % of the observed maximum efficiency for the first order of $\lambda(e_2(\lambda/2)/e_{1max} > 0.1)$. Hence Fig. 2 indicates those regions where the grating will insufficiently suppress the first higher harmonic. (The ratio $e_2(\lambda/2)/e_{1max}$ reaches 50 % at most.)

The performance of the monochromator BUMBLE BEE can be discussed successfully using Fig. 2 but additionally a number of monochromators that use quite similar grating parameters could also be examined and optimized with the help of this figure (GLEISPIMO /2/, FLIPPER /6,8/, BESSY SX700 /3/, UMO /9/, ERG /10/). In the mode where the selected λ is always in the blaze maximum

$\delta = \phi_{pre} - \phi_{grat} = 1°$ is constant. Here ϕ_{pre} and ϕ_{grat} are the grazing angles of incidence on the premirror and grating, respectively. The deviation from parallelity δ, is a parameter important also in further discussions. The BUMBLE BEE reaches its limit at E = 1220 eV in this mode with $\phi_{pre} = 2°$ and $\phi_{grat} = 1°$. Fixed $\delta = 1.0°$ operation is shown in Fig. 2 demonstrating that second order will be effectively suppressed at short wavelengths. For $\lambda > 3$ nm the first order efficiency is decreasing rapidly. $\delta = 1.5°$ is found to be optimal for the region 6 nm $\leq \lambda <$ 20 nm for both aspects: output and second order suppression. Problems occur for 3 nm $\leq \lambda \leq$ 6 nm, where still other values for δ have to be selected. Only the analysis for the two angles $\delta = 1.0°$ and $\delta = 1.5°$ is given in detail, the optimal regions are indicated in all the following figures by bars.

Equally important are the parameters of the premirror, which will be discussed for a gold coating. The reflectivity data measured between 1.6 nm and 10 nm are in good agreement with theoretical calculations taking the Fresnel equations for s-polarized light and using optical constants derivated from "atomic scattering factors" published by Henke et al. /11/. The best fit is obtained by introducing a RMS-roughness σ of 1 nm in the formula $R = R_0 \exp(-(4\pi\sigma\sin\phi/\lambda)^2)$ /12/ (ϕ is the glancing angle of incidence). The mirror was evaporated in HV and afterwards exposed to air for a long period. So the measured data are of practical importance because monochromator mirrors are often handled similarily. Theoretical isoreflectance curves for R = 0.3 and for $R(\lambda/2)/R(\lambda) = 0.3$, $\sigma = 0$ are shown in a $\phi(\lambda)$ diagram in Fig. 3. In the range 30 nm $\leq \lambda \leq$ 10 nm, the behaviour deviates considerably from the free electron gas behaviour. The curves on which the BUMBLE BEE is operated (Fig. 3) show, that the gold coated mirror introduces problems in the region where also the grating has low performance. Other coatings as Ni /11/ should be used for wavelengths around 5 nm.

3. Monochromator output

We calculate the normalized monochromator output $I_o(E)$ in photons/(s 100 mA current in DORIS 1 % bandwidth). For actual conditions $I_o(E)$ has to be scaled to the real current in DORIS and to the bandwidth accepted. The latter is achieved by multiplying $I_o(E)$ by s/s_o where s_o is a nominal slit width corresponding to a 1 % bandwidth as determined by the dispersion of the grating and s is the actual slit width. For a continuous spectrum the intensity measured behind the exit slit is not affected by any degradation of the achieved resolution due to source size, imaging errors of the paraboloid or defocussing. This affects only the spectral purity of the radiation passing through the slit.

For calculating $I_o(E)$ we need to calculate the spectral intensity of synchrotron radiation accepted by the monochromator, the reflectivity as a function of wavelength of all mirrors and the efficiency of the grating. Deflection mirror and toroid are Kanigen coated while the paraboloid and the grating are gold coated. Three premirrors can be changed in-situ, they are coated with Au, Kanigen and a 3-period Au/C multilayer. On a small blank a successful coating with a 3-period multilayer was achieved which gave enhancement of the reflectivity in the $\delta = 1.0°$ mode. Unfortunately due to errors in the evaporation process the large blank needed to cover the full spectral range was coated with a film with too thick layers and thus did not achieve the same good performance.

All calculations are based on the atomic scattering factors given by Henke et al. /11/ (for Kanigen the Ni-data are chosen). Surface roughness was taken into consideration with $\sigma_{RMS} = 1$ nm as found for the test mirror coated

with gold. All mirror reflectivities are calculated with the Fresnel-formalism (s-polarized). The multilayer film was calculated using recursion techniques given by Heavens /13/.

The most demanding calculation is that of the grating efficiency. There exists in principle the exact electromagnetic theory for a grating with an ideal profile as given by Petit /14/. Instead, we have used a semiempirical analytic expression which gave a good fit to the data obtained with the above mentioned FLIPPER grating. It gave the efficiency maximum at the correct angle. Near the maximum the deviations in the efficiency are less than 10 %. In regions where the efficiency is reduced by one order of magnitude deviations of the data can be as large as + 100 % to - 50 %. This parametrized form of the efficiency is a modification of the expressions given by Sprague et al. /15/ and Lukirski et al. /16/ and will be described elsewhere /17/.

The calculated intensities at the sample position are shown in Fig. 4. The measured data for the different configurations are derived from Au-diode currents that have been converted to photon intensities with the yield curves given by Lenth /18/ and Henke et al. /19/. Considering the large number of components involved (5 reflections) the agreement between calculation and measurement can be regarded as good. The measured data also agree quite well with the published estimate /1/ which was derived from a much simpler model taking optical constants given by Hagemann et al. /20/.

The largest values of the output were found with the multilayer coated pre-mirror for $\delta = 1.5°$ and $\delta = 2.0°$ at $E = 124$ eV. There the transmission of the whole set-up (monochromator and beam line) is 3 % and 8 % respectively.

4. False light

Not only the photons with the nominal wavelength will pass the exit slit. Stray light that will not correspond to the desired wavelength and higher orders that will fulfill the grating equation are admixed. The two contributions will be discussed separately.

A. Second order radiation

Only spectrally non-dispersive detectors are available in our reflectometer. Nontheless not only the amount of second order radiation present in the output but also the relative detection efficiency of the detector for first and second order light is of importance for the reflectometer measurements. The above discussed FLIPPER grating was used for a secondary analysis of the radiation. The procedure is quite similar to the method described by Källne et al. /21/, who used transmission gratings for an analysis of the output of the Grasshopper monochromator. The higher harmonics can be detected unambiguously between the zeroth order and the first orders. The quality of the grating with respect to scattered light in this range will determine the detection limit. The high photon flux at the sample did not allow to operate the multiplier detector (20 stage Johnson MM1 with Al_2O_3 coated (15 nm) pre-cathode) in the photon counting mode, so we had to measure the current from the last dynode, which is proportional to the second order photon intensity $I_{o,2}(\lambda/2)$, the grating efficiency $e(\lambda/2)$ and the detector sensitivity Y. If the grating is used in blaze maximum for the second order the signal is given by $Z(\lambda/2) = I_{o,2}(\lambda/2)\ e_B(\lambda/2)\ Y(\lambda/2)$. $e_B(\lambda/2)$ must be determined independently for blaze maximum conditions. With the signal $Z_o(\lambda)$ incident onto the grating the fraction of second order in the total signal is given by

$$V = \frac{I_{o,2}(\lambda/2)\ Y(\lambda/2)}{Z_o(\lambda)} = \frac{Z(\lambda/2)}{Z_o(\lambda)} \quad \frac{1}{e_B(\lambda/2)} \quad .$$

This ratio has to be very small for successful reflectivity measurements. Generally no second order contribution could be identified, third order was never detected for the two optimized configurations. The light scattered from the FLIPPER grating leads to the detection limit shown in Fig. 5. Also indicated are the ratios V for a gold premirror. Calibrating the multiplier detector against the signal from the Au-diode we can finally deduce the second order contributions as given in Table 2. These measurements demonstrate the proper choice of the parameters δ as discussed above.

B. Stray light

The stray light contribution cannot be derived as an absolute photon intensity. The measurements on the FLIPPER grating shows that this stray light consists of light with longer wavelengths than the selected one. This unwanted signal can only be determined experimentally for each type of detector. Because of the long wavelengths involved stray light leads to too large values of angle dependent reflectivities at large steep angles of incidence. This "remaining reflectivity" gives an estimate of the false light. The errors are large (+ 100 % ... - 50 %). The detection limit lies in the order of a few %, so that only a few points could be measured. The results are shown in Fig. 6 in comparison with the detected total signal and with the second order contribution. It is obvious that in some intervals the stray light will dominate the false light signal. With $\delta = 0.8°$ the stray light level at E = 1500 eV (λ = 0.8 nm) attains 50 %. The stray light levels will sometimes make impossible reliable reflectivity measurements, however, grating efficiency data can still be derived after a stray light correction. The intervals indicated as optimal in the figures will show false light con-

tributions of less than 1 % in the multiplier detector. Thus only the region 3 nm $\leq \lambda \leq$ 6 nm is difficult to use.

5. Resolution

The short distance of the monochromator from the source point will cause aberrations on the extreme off-axis paraboloid /22/. Additionally the divergent radiation incident onto the grating will lead to astigmatism according to Murty /23/ caused by different virtual distances of the source point for vertical and for horizontal focussing due to the change of the vertical divergence at the grating. The resolution is among others determined by the size of the vertical focus. In order to follow the varying focal length the exit slit is mounted between two bellows and movable on a 60 mm track along the beam. For standard reflectivity measurements it is not advisable, however, to follow the focus continuously while scanning the spectrum since the subsequent toroid (see Fig. 1) which re-focusses the beam on the detector requires a fixed source point.

Simple geometrical optics is insufficient to determine the best compromise position for our spectral range. For this optimization a ray tracing program according to the scheme given by Spencer and Murty /24/ was written. An extension of the program allows to calculate the energy resolution /17/.

In order to determine the resolution experimentally the absorption fine structures of gases were measured in an ionisation chamber described by Eberhardt et al. /25/ in order to make an accurate wavelength calibration. Some of these structures which are given in Table 3 allow to determine the resolution because of their small inherent width. The measured resolution as given in Fig. 7 is compared to ray tracing calculations. These calculations

were made for ideally shaped components. Shape errors mainly of the paraboloid in the order of 2.5" will additionally broaden the image of the source at the exit slit leading to reduced resolution so that the observed mean deviation of only 35 % between theory and experiment is reasonable. It indicates a good alignment of the whole equipment.

It is, however, possible to achieve a better resolution. This is shown in Fig. 8. Caused by the wrong exit slit position neither an increased δ (δ = 2.5°) nor a smaller horizontal acceptance (6 mm) for the reduction of astigmatism can enhance the resolving power. Only the correct slit position in connection with the other measures will lead to the considerably improved resolution $\Delta E/E$ = 1/500 at 250 eV photon energy.

Conclusion

We have demonstrated that by a detailed knowledge of grating efficiencies and reflectivities of optical components it is possible to plan a special purpose grazing incidence monochromator not only with respect to its resolving power but also with respect to its output characteristics and rejection of higher orders. The measurements on the instrument show that it achieves its predicted performance in considerable detail. Accurate reflectivity measurements are now possible between 1.5 nm and 26 nm. The range above 26 nm will be covered by a new grating with 300 lines/mm in the future. The range from 0.8 - 1.5 nm is still usuable but care has to be taken with stray light there.

Acknowledgement

We want to thank R.P. Haelbich, H. Hogrefe, D. Giesenberg and A. May for their support during the construction and installation of the monochromator. The very accurate work done on the different components of the monochromator in the workshops of DESY and the II. Institut für Experimentalphysik is gratefully acknowledged. This work was supported by the Bundesministerium für Forschung und Technologie under contract no. 05 248 Ku.

References:

/1/ W. Jark, R.-P. Haelbich, H. Hogrefe und C. Kunz, Nucl. Instr. and Meth. 208, 315 (1983)

/2/ H. Dietrich und C. Kunz, Rev.Sci.Instrum. 43, 434 (1972)

/3/ H. Petersen und H. Baumgärtel, Nucl. Instr. and Meth. 172, 191 (1980)
F. Riemer und R. Torge, Nucl. Instr. and Meth. 208, 313 (1983)

/4/ H. Petersen, Opt. Commun. 40, 402 (1982)

/5/ H. Hogrefe, D. Giesenberg, R.-P. Haelbich und C. Kunz, Nucl. Instr. and Meth. 208, 415 (1983)

/6/ W. Eberhardt, G. Kalkoffen und C. Kunz, Nucl. Instr. and Meth. 152, 81 (1978)

/7/ J. Barth, F. Gerken, C. Kunz und J. Schmidt-May, Nucl. Instr. and Meth. 208, 307 (1983)

/8/ R. L. Johnson und J. Reichardt, Nucl. Instr. and Meth. 208, 791 (1983)

/9/ F. C. Brown und S. L. Hulbert, Nucl. Instr. and Meth. 222, 42 (1984)

/10/ S. L. Hulbert, J. P. Stott, F. C. Brown und N. C. Lien, Nucl. Instr. and Meth. 208, 43 (1983)

/11/ B. L. Henke, P. Lee, T. J. Tanaka, R. L. Shimabukuro und B. K. Fujikawa, At. Dat. Nucl. Dat. Tables 27, 1 (1982)

/12/ P. Beckmann und A. Spizzichino, The Scattering of Electromagnetic Waves from Rough Surfaces (Pergamon Press Ltd. New York 1963)

/13/ O. S. Heavens, Optical Properties of Thin Solid Films (Dover Publications, Inc., New York 1965)

/14/ R. Petit, ed., Electromagnetic Theory of Gratings, Topics in Current Physics 22, (Springer Verlag, Berlin 1980)

/15/ G. Sprague, D.H. Tomboulian und D. E. Bedo, J. Opt. Soc. Am. 45, 756 (1955)

/16/ A. P. Lukirskii und E. P. Savinov, Opt. Spectrosc. 14, 147 (1963)

/17/ W. Jark, Thesis in preparation, Hamburg University 1985

/18/ W. Lenth, Diplomarbeit, Universität Hamburg 1975
Interner Bericht DESY F41-75/07
presented in
C. Kunz, Synchrotron Radiation, Topics in Current Physics 10, Springer Verlag Heidelberg 1978, Page 135

/19/ B. L. Henke, J. P. Knauer und K. Premaratne, J. Appl. Phys. 52, 1509 (1981)

/20/ H.-J. Hagemann, W. Gudat und C. Kunz, DESY-Report SR 74-7, 1974

/21/ E. Källne, J.H. Dijkstra, R. Bartlett, T. Kitchens, R.O. Tatchyn, M. Hecht und I. Lindau, Reflecting Optics for Synchrotron Radiation, Proc. SPIE 315, 178 (1981)

/22/ H. Wolter, Ann. Physik 10, 94 (1952)

/23/ M. V. R. K. Murty, J. Opt. Soc. Am. 52, 768 (1962)

/24/ G. H. Spencer und M. V. R. K. Murty, J. Opt. Soc. Am. 52, 672 (1962)

/25/ W. Eberhardt, R.-P. Haelbich, M. Iwan, E. E. Koch und C. Kunz, Chem. Phys. Letters 40, 180 (1976)

/26/ M. Nakamura, Y. Morida, T. Hayaishi, E. Ishiguro und M. Sasanuma, Conf. Digest III. Intern. Conf. on VUV Radiation Physics, Editor: Y. Nakai, Tokyo 1971, S. 1pA1-6

/27/ M. Nakamura, M. Sasanuma, S. Sato, M. Watanabe, H. Yamashita, Y. Iguchi, A. Ejiri, S. Nakai, S. Yamaguchi, T. Sagawa, Y. Nakai und T. Oshia, Phys. Rev. 178, 80 (1969)

/28/ M. Nakamura, M. Sasanuma, S. Sato, M. Watanabe, H. Yamashita, Y. Iguchi, A. Ejiri, S. Nakai, S. Yamaguchi, T. Sagawa, Y. Nakai und T. Oshia, Phys. Rev. Lett. 21, 1303 (1968)

/29/ K. Codling und R. P. Madden, Phys. Rev. Lett. 12, 106 (1964)

Table 1: Dimensions of the optical components

component	size		material	coating	angle of incidence	manufacturer
	length x width (mm)	optically accurate				
PM1: defl. mirror	330 x 65	330 x 65	Cu	Kanigen	2°	Zeiss
PM: premirror	155 x 30	150 x 20	Al zerodur	Kanigen 30 nm Au	*	Zeiss
PG: plane grating blazed γ=1.0°	155 x 30	145 x 24	zerodur quartz	3 P Au/C 20 nm Au	* **	Zeiss ASTRON
P: paraboloid	250 x 60	200 x 20	zerodur	30 nm Au	2°	Zeiss
T: toroid	100 x 25	60 x 10	Al	Kanigen	2°	Zeiss

* variabel: 2° - 45°
** variabel: 1° - 60°
3 P Au/C: 3 periods of 15.2 nm Au and 8.5 nm C on 20 nm Au

Table 2: Second order photon intensities at the sample for the two optimized operating configurations of the BUMBLE BEE.
Total intensity I_{tot} = 100% (error: +100% .. -50%)

λ in nm		$I_2(\lambda/2)/I_{tot}$	
		δ = 1.0°	δ = 1.5°
1.6		< 1.0% n	< 1.0% n
2.2		< 1.0% n	3.0%
3.2		< 0.2% n	8.0%
4.5	Au	0.2%	5.0%
	multil	0.4%	9.0%
	kanigen	< 0.1%	1.7%
6.5	Au	< 0.1% n	1.1%
	multil	0.2%	6.7%
	kanigen	< 0.1%	1.1%
9.0	Au	< 0.1% n	< 0.1% n
	multil	< 0.1% n	0.2%
	kanigen	< 0.1%	0.2%
13.0		< 0.1% n	< 0.1% n
18.0		< 0.1% n	< 0.1% n
26.0			0.7%

n = no second order identified .

Table 3: Structures measured to determine the resolution and to check the calibration

Gas	structure	λ in nm	ref.	remarks
O_2	$\sigma_u 1s \rightarrow (\pi_g 2p)^3$	2.33	/26/	★
N_2	$\sigma_u 1s \rightarrow \pi_g 2p$	3.093	/27/	★
Ar	2p → 4s	5.071	/28/	
Kr	3d → 5p	13.588	/29/	
Xe	4d → 6p	19.041	/29/	

★ at δ = 1.5° and δ = 2.0° also detected in 2. order

Figure Captions

Fig. 1: Schematic diagram of the beamline G1 with the monochromator BUMBLE BEE (components not drawn to scale):

PM1: deflection mirror — EA: entrance aperture
PM: plane premirror — PG: plane grating
P: paraboloid — ES: exit slit
T: toroid — D: diaphragm
S: sample — Det: detector

Fig. 2: Extended grating efficiency map for a blazed Au-grating (1.5° blaze angle, 1200 grooves/mm) with:
e_{1max}: first order efficiency maximum
$e_{1max}/2$: 50 % level of e_{1max}
e_2: efficiency of the second order of λ/2
δ = 1.° and δ = 1.5°: working curve of the monochromator
opt.: regions where the second order is efficiently suppressed

Fig. 3: Premirror reflectivity map for Au-mirror,
a) isoreflectivity curve for 30 % reflectivity R(λ)
b) second order suppression curve for R(λ/2) = 30 % R(λ).
Below both curves the values will increase.

Fig. 4: Intensity on the sample for standard configurations of the BUMBLE BEE for all possible combinations compared to the calculated performance (points).

Fig. 5: Ratio of signal caused by second order to total signal using a Au-coated premirror and a photomultiplier detector with Al_2O_3 cathode for the two standard configurations.

Fig. 6: Comparison between total signal, contribution of stray light and second order for the $\delta = 1.0°$ mode. For comparative purposes the total signal is also shown for the $\delta = 1.5°$ mode where the stray light signal will be practically the same as indicated while the second order contribution differs considerably (see Fig. 5).

Fig. 7: Calculated and experimental resolving power of the monochromator for 3 different simultaneous rotation modes. Exit slit fixed at b = 1025 mm with 30 µm width.

Fig. 8: Absorption fine structure measured at the argon-L-edge in different configurations compared with the data of ref. /28/.

Fig. 1

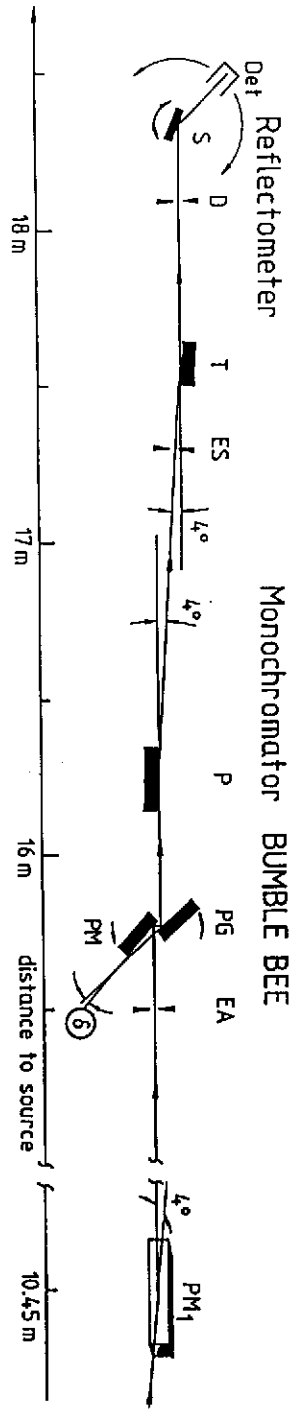

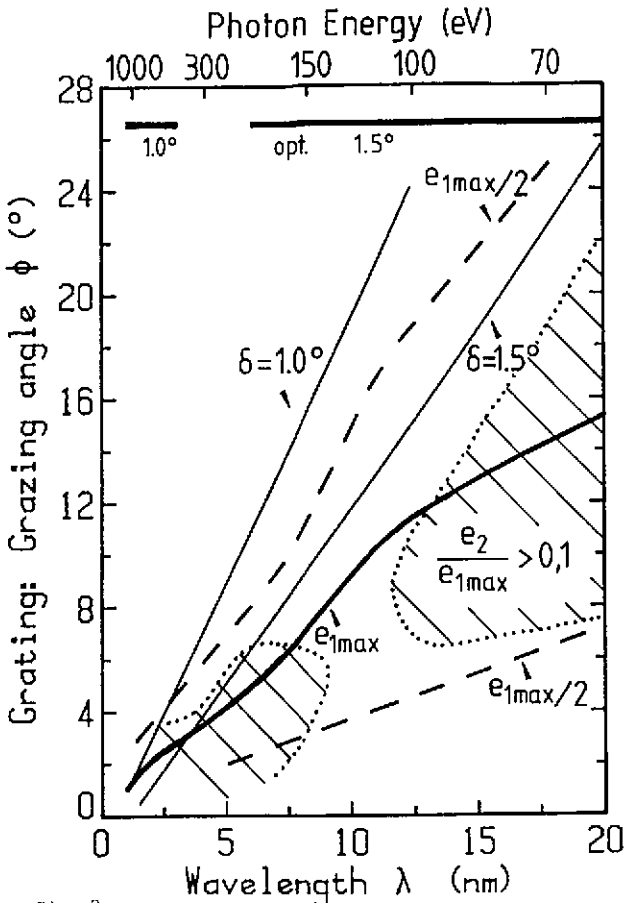
Photon Energy (eV)
1000 300 150 100 70
1.0°
opt. 1.5°
$e_{1max}/2$
δ=1.0°
δ=1.5°
$\frac{e_2}{e_{1max}} > 0,1$
e_{1max}
$e_{1max}/2$
Grating: Grazing angle φ (°)
Wavelength λ (nm)

Fig. 2

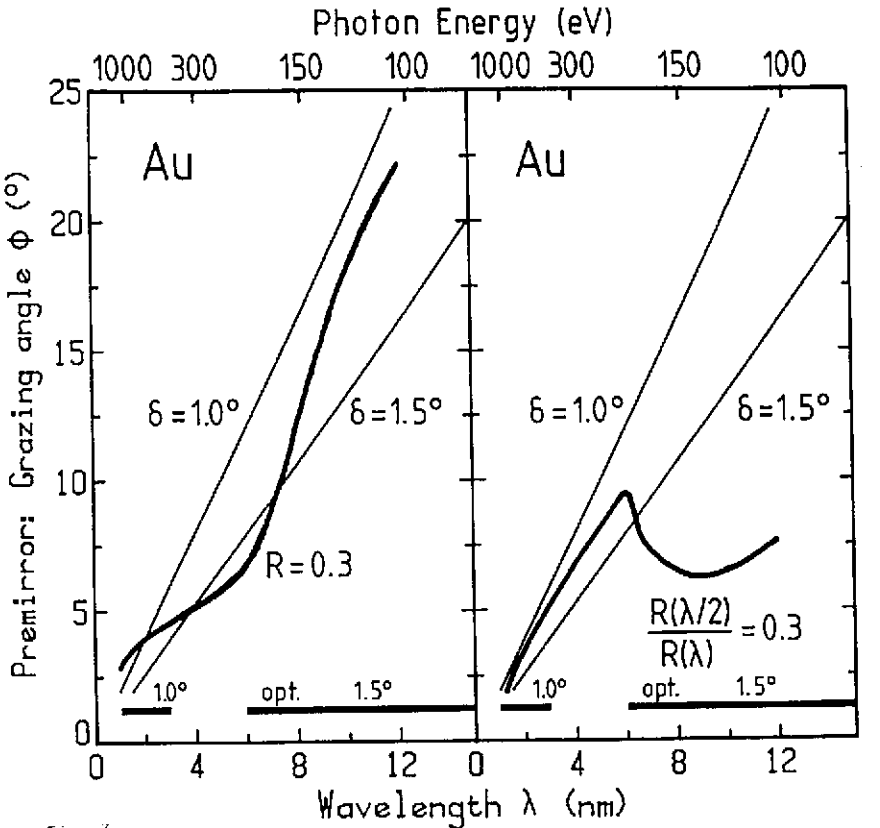
Photon Energy (eV)
1000 300 150 100 1000 300 150 100
Au
Au
δ=1.0°
δ=1.5°
R=0.3
$\frac{R(\lambda/2)}{R(\lambda)} = 0.3$
1.0°
opt. 1.5°
Premirror: Grazing angle φ (°)
Wavelength λ (nm)

Fig. 3

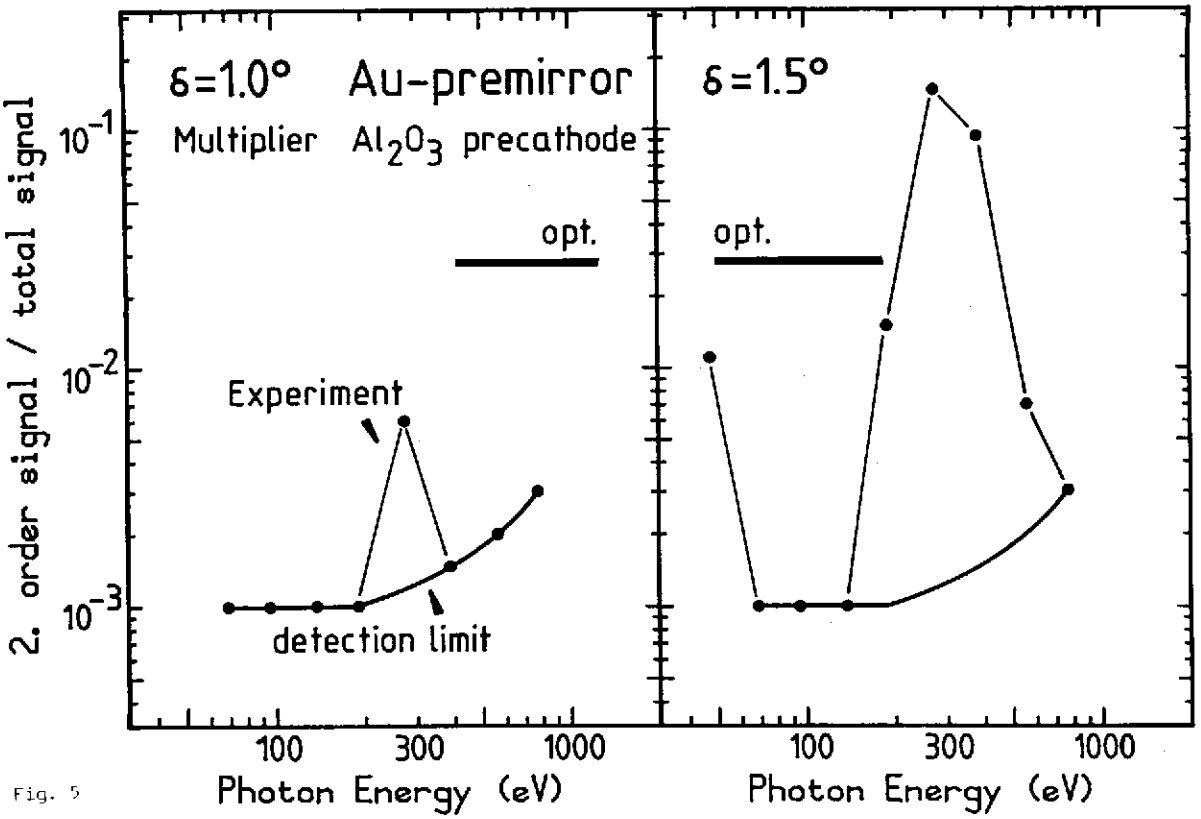
δ=1.0° Au-premirror
Multiplier Al_2O_3 precathode
opt.
Experiment
detection limit
δ=1.5°
opt.
2. order signal / total signal
10^{-1}
10^{-2}
10^{-3}
100
300
1000
Photon Energy (eV)
Photon Energy (eV)

Fig. 5

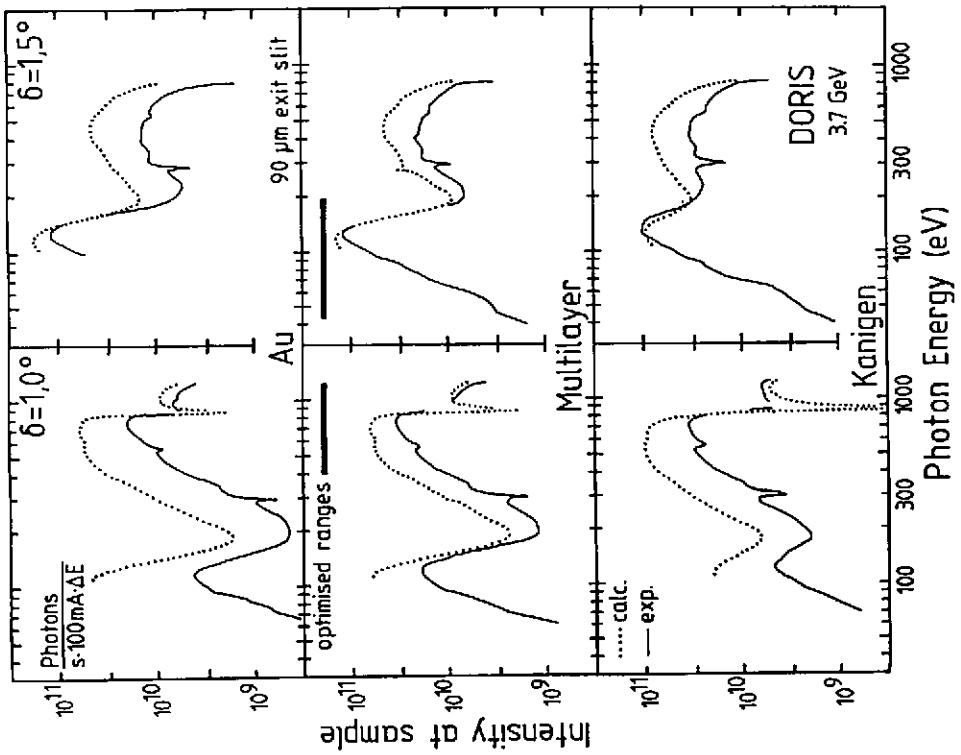
δ=1,5°
δ=1,0°
90 µm exit slit
optimised ranges
Au
Multilayer
Kanigen
DORIS
3.7 GeV
Photons
s·100mA·ΔE
..... calc.
— exp.
Intensity at sample
10^{11}
10^{10}
10^{9}
100
300
1000
Photon Energy (eV)

Fig. 4

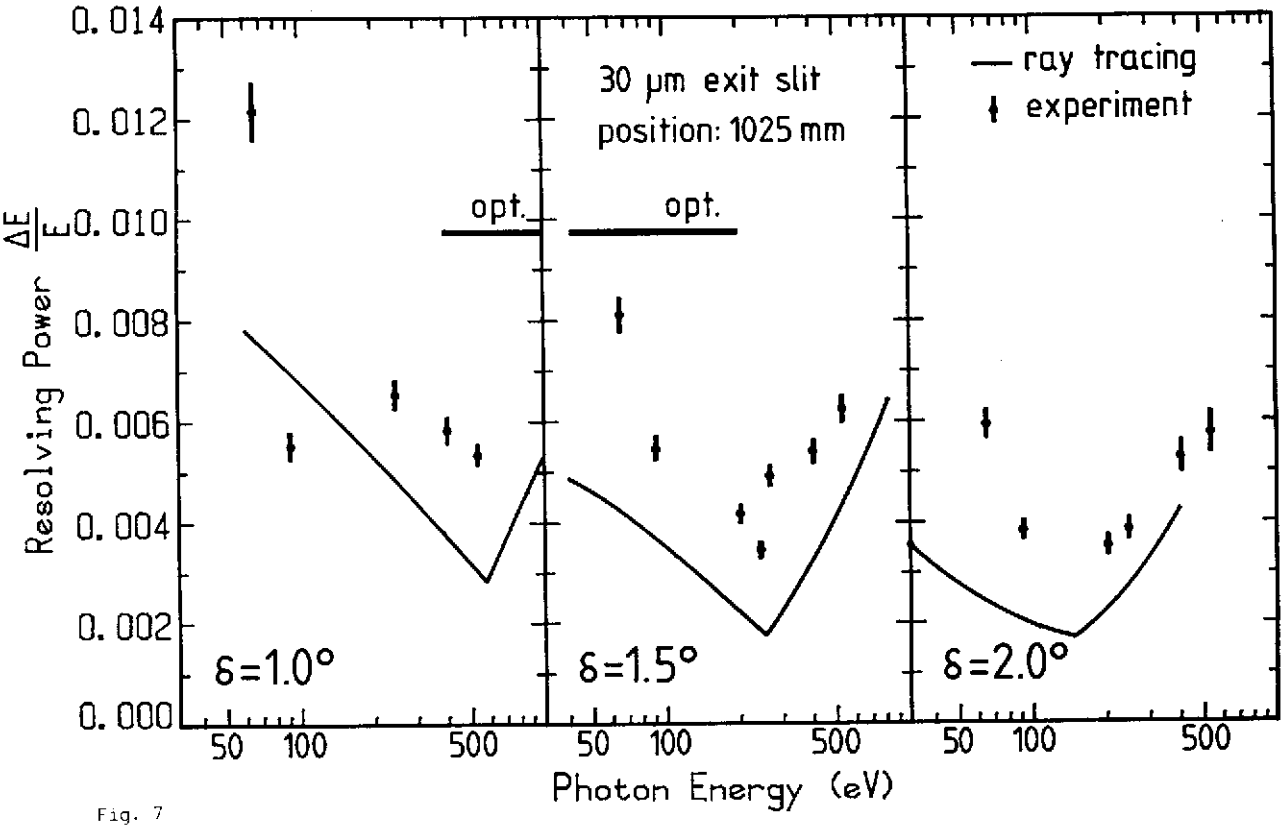
0.014
0.012
0.010
0.008
0.006
0.004
0.002
0.000
Resolving Power $\frac{\Delta E}{E}$
30 µm exit slit
position: 1025 mm
ray tracing
experiment
opt.
opt.
δ=1.0°
δ=1.5°
δ=2.0°
50
100
500
Photon Energy (eV)

Fig. 7

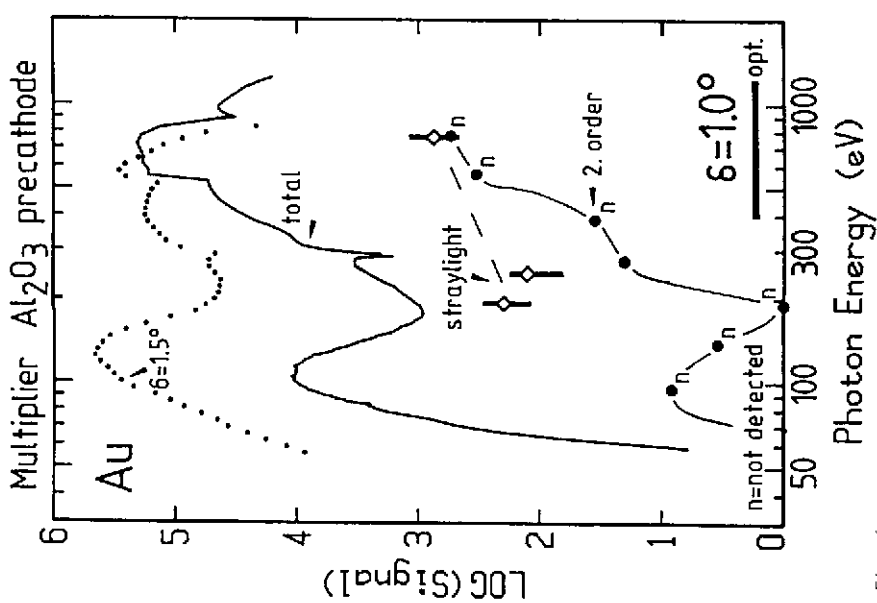
Multiplier Al_2O_3 precathode
Au
δ=1.5°
total
straylight
2. order
δ=1.0°
opt.
n=not detected
LOG (Signal)
Photon Energy (eV)
50
100
300
1000

Fig. 6

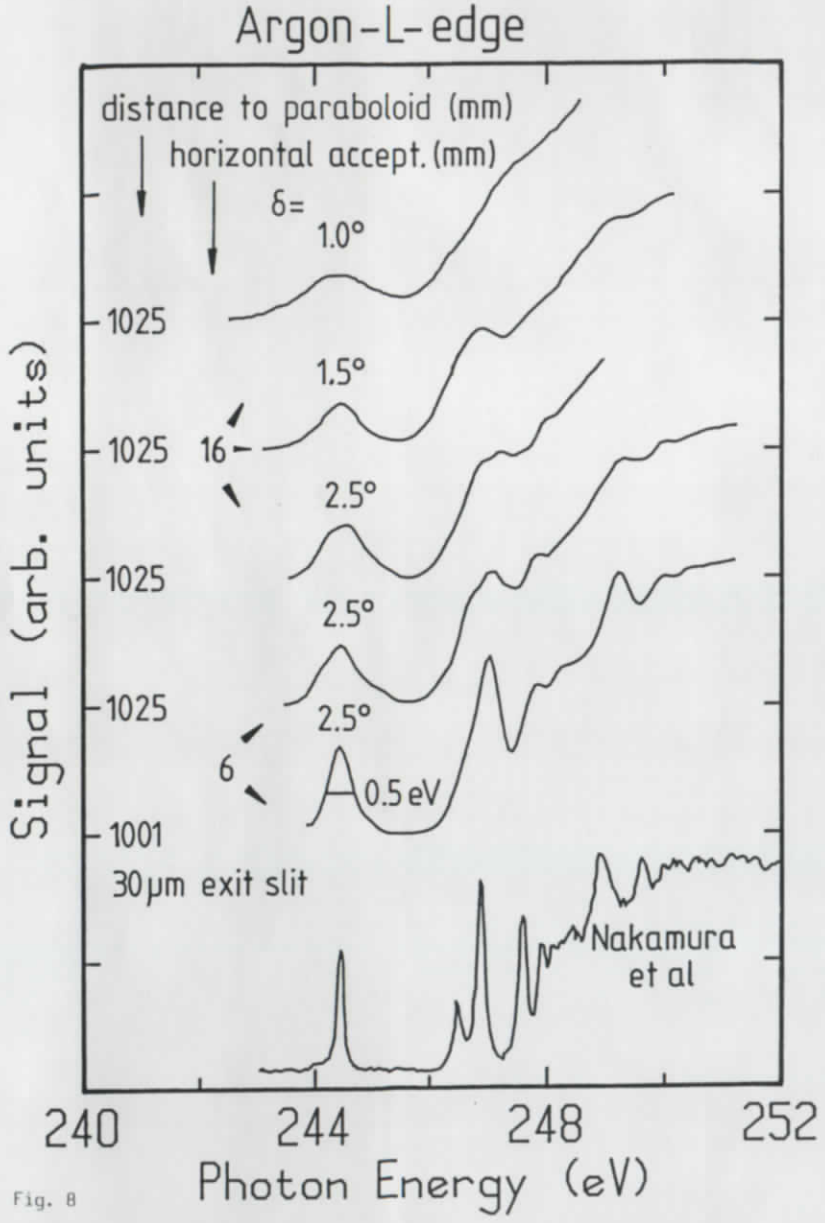
Argon-L-edge
distance to paraboloid (mm)
horizontal accept. (mm)
δ=
1.0°
1.5°
2.5°
2.5°
2.5°
1025
1025
1025
1025
1001
16
6
0.5 eV
30 μm exit slit
Nakamura et al
Signal (arb. units)
240
244
248
252
Photon Energy (eV)

Fig. 8